

RSC Advances



This is an *Accepted Manuscript*, which has been through the Royal Society of Chemistry peer review process and has been accepted for publication.

Accepted Manuscripts are published online shortly after acceptance, before technical editing, formatting and proof reading. Using this free service, authors can make their results available to the community, in citable form, before we publish the edited article. This *Accepted Manuscript* will be replaced by the edited, formatted and paginated article as soon as this is available.

You can find more information about *Accepted Manuscripts* in the [Information for Authors](#).

Please note that technical editing may introduce minor changes to the text and/or graphics, which may alter content. The journal's standard [Terms & Conditions](#) and the [Ethical guidelines](#) still apply. In no event shall the Royal Society of Chemistry be held responsible for any errors or omissions in this *Accepted Manuscript* or any consequences arising from the use of any information it contains.

COMMUNICATION

Needle-like CoO Nanowires Grown on Carbon Cloth for Enhanced Electrochemical Properties in Supercapacitors

Cite this: DOI: 10.1039/x0xx00000x

Received 00th January 2012,
Accepted 00th January 2012D. L. Ji,^{a,b,d} J. H. Li,^{c*} L. M. Chen,^{a*} D. Zhang,^a T. Liu,^a N. Zhang,^b R. Z. Ma,^b G. Z. Qiu^a and X. H. Liu^{a,b,d*}

DOI: 10.1039/x0xx00000x

www.rsc.org/

Needle-like CoO nanowires grown on carbon cloth have been successfully fabricated by a controllable hydrothermal method followed via annealing process. The as-fabricated nanostructure showed enhanced specific capacitances and excellent cycling stability in supercapacitors.

With increasing energy demand on energy-storage devices, supercapacitors (SCs) are considered as one of the most promising power devices because of the superior operating lifetimes, better safety, and faster charge discharge capability.¹ Many transition metal oxides and hydroxides have been chosen as electrode materials to increase the storage performance of pseudocapacitors, such as RuO₂,² NiO,³ CoO_x,⁴ MnO₂,⁵ Ni(OH)₂,⁶ Co(OH)₂,⁷ and so on. Among these materials, cobalt oxides are cheap materials with high theoretical capacitances, which have attracted immense attention during the past few decades.⁸ Especially, cobalt monoxide (CoO), with a higher theoretical capacitance than cobalt oxide (Co₃O₄), is a promising candidate for pseudocapacitor electrode materials.⁹ However, the poor electrical/ionic conductivity of CoO caused the low specific capacitance, which hinders the future applications in SCs. Thus, to improve the electrochemical performances for CoO in SCs is still a sophisticated challenge.

SCs with high energy density require that the electrode materials must possess sufficient surface electro-active species and facilitate the transition of electrons for Faradaic redox reactions.^{1a} Due to the good electron transportation capability, high surface-to-volume ratio, and relatively lower volume expansion-contraction during the charge discharge process compared with the bulk materials, one-dimensional (1D) nanostructures have been widely selected as efficient nanostructure for the electrochemical electrodes.¹⁰ However, for CoO materials, although the 1D CoO is selected as enhanced electrode materials, the experimental capacitance ability is still low in comparison with Co₃O₄.¹¹ Recently, in order to further increase the transition of electrons, well-designed 1D nanoarrays of metal oxides directly grown on conductive substrates were used as binder-free electrodes for SCs. For example, Guan et al. have reported a high specific capacitance of well-aligned CoO nanowire array freely standing on Ni foam substrate.¹²

However, Xing et al. successfully demonstrated that using nickel foam as current collector can bring about substantial errors to the specific capacitance values of electrode materials.¹³ Rakhi et al. have reported the synthesis of self-organization Co₃O₄ nanowires on carbon fiber paper and planar graphitized carbon paper, respectively.¹⁴ In comparison, self-organization Co₃O₄ nanowires grown on carbon fiber paper showed better electrochemical performance than that grown on planar graphitized carbon paper. Compared with planar substrate, carbon fiber paper (CFP) or carbon cloth (CC) with a network structure has large surface area, high porosity and good electric conductivity. Furthermore, it can be used in harsh environments such as folding/twisting conditions.¹⁵ So, well designed 1D CoO nanostructure on CC seems a promising candidate for enhanced electrode materials in SCs.

In current work, needle-like CoO nanowires grown on CC was fabricated via a controllable hydrothermal method followed by thermal treatment. The as-fabricated hierarchical structures were used as binder-free electrode for SCs, which exhibited the highest specific capacitance compared with Co₃O₄ nanowires/CC, CoO nanosheets/CC, and nanowire-assembled CoO microspheres. The synthetic process is illustrated in Scheme S1 (ESI†). Firstly, the CC was vertically inserted into mixed solution of Co(NO₃)₂·6H₂O, NH₄F and urea. After the hydrothermal process, well defined needle-like precursor indexed as Co(CO₃)_{0.5}(OH)·0.11H₂O (JCPDS 48-0083) can be easily grown on the highly flexible CC (see Fig. S1, ESI†). Finally, the precursor was completely converted into cobalt oxides (CoO and Co₃O₄) supported on the CC by heat treatment at 450 °C in high-purity Ar gas ambient and/or at 350 °C in air for 2 h, respectively. More importantly, as-transformed cobalt oxides could retain the original morphological features.

Fig. 1A shows the X-ray diffraction (XRD) pattern of as-prepared needle-like CoO nanowires/CC product obtained by calcination of needle-like precursor on CC at 450 °C for 2 h under argon flow. The peaks at about 24° and 44° are attributed to the CC substrate.¹⁶ Other diffraction peaks can be readily indexed as a cubic structure with lattice constant *a* = 0.426 nm, in good agreement with the standard data for CoO (JCPDS 43-1004). Fig. 1B depicts the low-magnification scanning electron microscopy (SEM) image of as-prepared product, revealing the

ordered woven structure of the CC templates kept unchanged after the deposition process (see Fig. S2, ESI†). The high-magnification SEM image shown in Fig. 1C clearly reveals that each carbon fiber is covered with numerous highly ordered CoO nanowires. Further magnified SEM image is displayed in Fig. 1D, which confirms abundant CoO nanowires, grown tidily on the surface of the carbon fibers, possesses a regular needle-like shape. The needle-like objects have an average bottom diameter of about 50 nm and tip diameter of approximate 20 nm, whereas a length up to 5 μm . Fig. 2E depicts a typical transmission electron microscopy (TEM) image of an individual CoO nanowire, which indicates that needle-like CoO nanowire is composed of many pore structures due to the pyrolysis and dehydration during calcination. In the inset, the corresponding selected area electron diffraction (SAED) pattern can be well indexed to cubic CoO, revealing a polycrystalline nature of the needle-like CoO nanowire. The high-resolution TEM (HRTEM) image of an individual CoO nanowire, as shown in Fig. 1F, demonstrates the interlayer spacing is measured to be 0.245 nm, which agrees well with the separation between (111) lattice planes of cubic CoO.

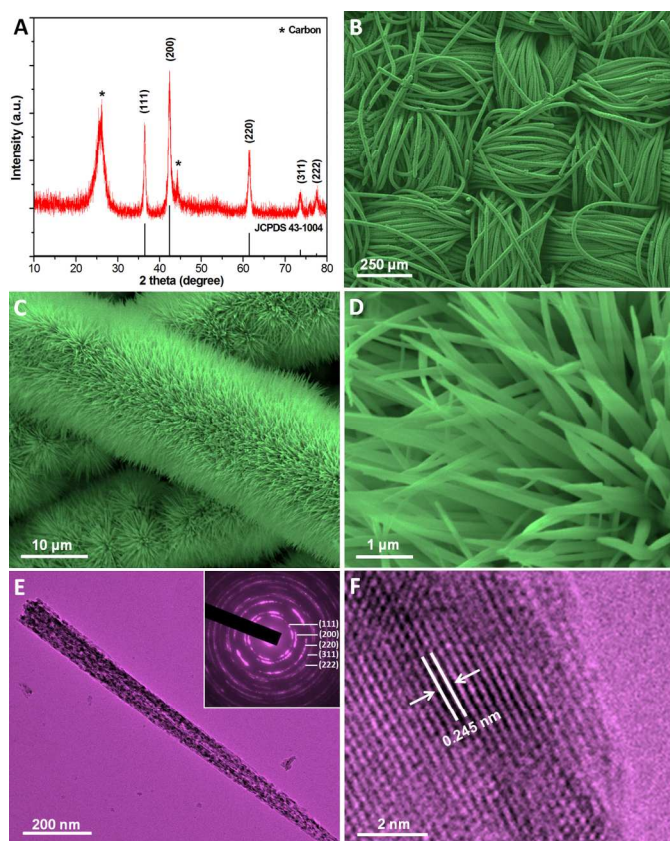


Fig. 1 (A) XRD pattern of as-prepared product obtained by calcination of the precursor on CC at 450 $^{\circ}\text{C}$ for 2 h under argon flow. (B-D) SEM images of as-prepared needle-like CoO nanowires/CC product. The inset in (E) shows an SAED pattern taken on the individual CoO nanowire.

On the other hand, the precursor could also be transformed into spinel Co_3O_4 at a temperature as low as 350 $^{\circ}\text{C}$ in air for 2 h, which would endow their potential application in various fields (see Fig. S3, ESI†). More importantly, as-transformed Co_3O_4 could retain the original morphological features, in good agreement with the structure for needle-like CoO nanowires supported on the CC, as shown in Fig. A and B. It is well

known that the morphology and size of the products strongly depend on the synthetic parameters. In particular, lamellar precursor could be prepared with the absence of NH_4F during the hydrothermal process, which could be more readily calcined into CoO at 450 $^{\circ}\text{C}$ for 2 h under argon flow (see Fig. S3, ESI†). Fig. 2A and B depicts typical SEM images of the CoO product obtained by calcination of lamellar precursor under argon flow. It is clearly seen that the lamellar structures aligned on CC are obvious. The 2D objects were crystallized into well-shaped and rectangular nanosheets of $5 \times 2.5 \mu\text{m}^2$. Furthermore, CoO microspheres could be obtained without the substrate of CC during the synthetic process (see Fig. S3, ESI†). As is shown in Fig. 2E and F, the needle-like nanowire with mean diameters of about 50 nm and length about 10 μm assembled and formed hierarchical CoO microspheres, longer than that of needle-like CoO nanowires/CC product. The average diameter of CoO microspheres was estimated to be about 20 μm .

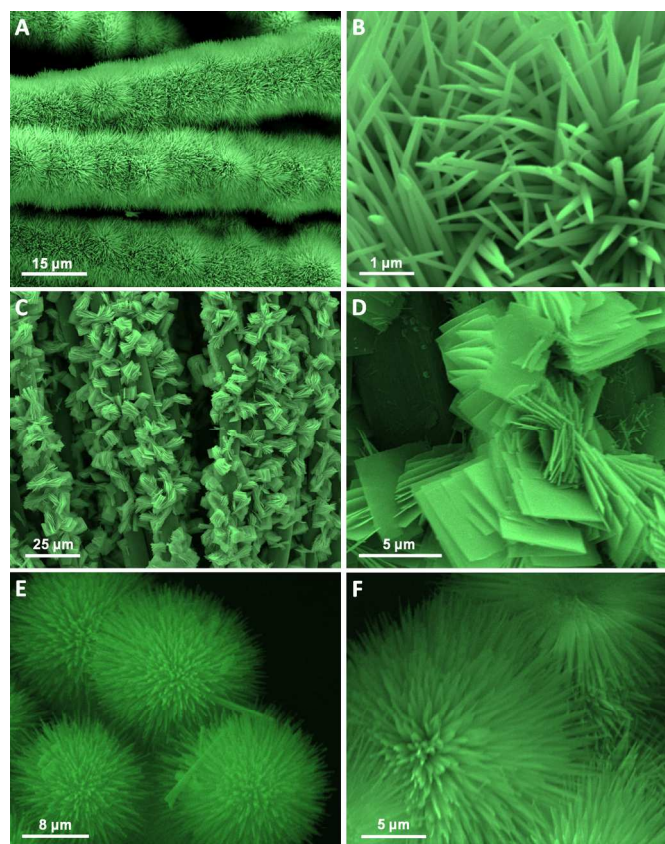


Fig. 2 (A, B) SEM images of needle-like Co_3O_4 nanowires/CC product calcined at 350 $^{\circ}\text{C}$ in air. (C, D) SEM images of rectangular CoO nanosheets/CC product obtained with the absence of NH_4F during the hydrothermal process and then calcined at 450 $^{\circ}\text{C}$ under argon flow. (E, F) SEM images of nanowire-assembled CoO microspheres obtained without the substrate of CC calcined at 450 $^{\circ}\text{C}$ under argon flow.

To evaluate the electrochemical performance of as-obtained products, cycle voltammetry (CV) and galvanostatic charge-discharge (CD) measurements were carried out in 2 M KOH aqueous electrolyte using a three electrodes system at room temperature. The needle-like CoO nanowires/CC product was directly used as electrode. For comparison purpose, Co_3O_4 nanowires/CC electrode, CoO nanosheets/CC electrode, and needle-like nanowire-assembled CoO microspheres electrode made by the traditional slurry-coating technique were also evaluated (see detailed experimental processes, ESI†). Fig. 3A

exhibits the typical CV curves of the above electrodes in a potential range of -0.2 to 0.5 V (vs Ag/AgCl) at a scan rate of 20 mV s^{-1} . The needle-like CoO nanowires/CC electrode has the largest CV area compared with other electrodes, which suggests that the needle-like CoO nanowires/CC electrode has the highest specific capacitance among these electrodes. Fig. 3B displays the galvanostatic charge–discharge curves of the above electrodes measured in the potential range between 0 and 0.45 V at a current density of 1 A g^{-1} . The specific capacitance could be calculated from the galvanostatic charge–discharge curves using the equation: $C = I\Delta t/m\Delta V$, where I is charge–discharge current, Δt is the time for a full discharge, m indicates the mass of the active material, and ΔV represents the voltage change after a full discharge.¹⁷ The specific capacitances are approximate 311.8 , 135.1 , 135.1 , and 97.17 F g^{-1} for needle-like CoO nanowires/CC, Co_3O_4 nanowires/CC, CoO nanosheets/CC, and nanowire-assembled CoO microspheres electrodes, respectively. Needle-like CoO nanowires/CC electrode possesses the highest specific capacitance, agreeing well with the CV profiles. Compared with Co_3O_4 , it probably originates from the fact that CoO has a higher theoretic capacitance. In addition, the specific capacitances of needle-like CoO nanowire/CC electrode are superior to those of rectangular CoO nanosheets/CC electrode, which are directly related with the nanowires with prominent capillary pathways and good electron transportation capability.¹⁰ Furthermore, the needle-like CoO nanowires supported on the CC also exhibited enhanced specific capacitance than the nanowire-assembled CoO microspheres, which is attributed to that the CoO nanowires directly grown on the CC with robust adhesion ensure intimate contacts and effective electron transport between the CC and the every nanowire. Besides, loose textures of substrates and large open spaces between neighboring nanowires making more active material exposed to the electrolyte that allow the electrolyte to easily contact with the CoO nanocrystals, providing hierarchical pathways for effective ion transport.^{15b, 18}

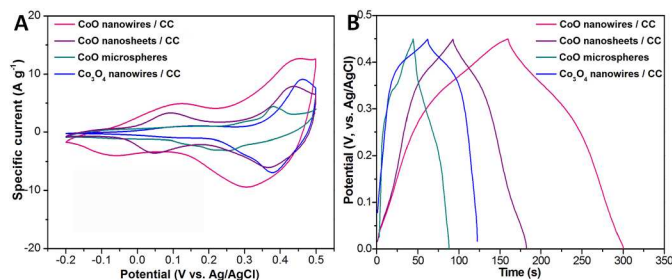


Fig. 3 (A) CV curves of CoO nanowires/CC, CoO nanosheets/CC, CoO microspheres, and Co_3O_4 nanowires/CC electrodes at the same scan rate of 20 mV s^{-1} . (B) Galvanostatic charge–discharge curves of CoO nanowires/CC, CoO nanosheets/CC, CoO microspheres, and Co_3O_4 nanowires/CC electrodes at the same current density of 1 A g^{-1} .

The detailed electrochemical performance of needle-like CoO nanowires/CC electrode was further studied. Fig. 4A indicates the typical CV curves of the needle-like CoO nanowires/CC electrode in three electrode configuration at different scan rates. The well-defined redox peaks within -0.2 – 0.5 V appear in all CV curves, which indicates that the electrochemical capacitance of as-prepared CoO products is derived from quasi-reversible Faradaic redox reactions.⁴ With increasing scan rate, the shape of the CV changed. The anodic and cathodic peak potential shift in more anodic and cathodic directions, respectively. This slight shift in the peak positions is

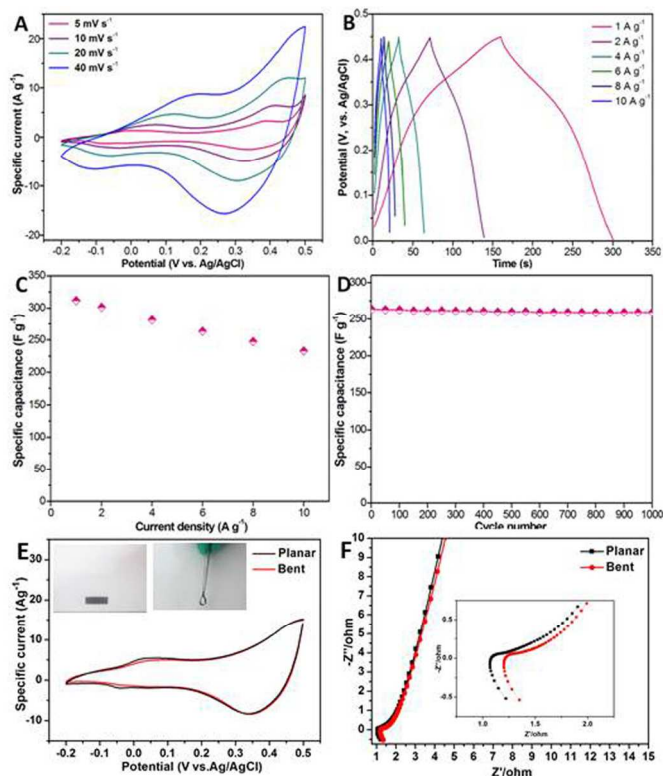


Fig. 4 (A) The CV curves of the needle-like CoO nanowires/CC product at different scan rates of 5 , 10 , 20 , and 40 mV s^{-1} . (B) Charge–discharge behavior at different current densities. (C) The corresponding specific capacitance at different current density. (D) Specific capacitance versus cycle number of as-prepared product at a galvanic charge and discharge current density of 6 A g^{-1} . (E) CV curves of the needle-like CoO nanowires/CC electrodes at a planar state and the bending state under a scan rate of 20 mV/s , the insets are the pictures of hybrid electrode under different state. (F) Nyquist plot for the needle-like CoO nanowires/CC electrodes at a planar state and the bending state. The inset is an enlarged curve of the high frequency region.

due to the fact that at lower scan rate electrolyte ions are fully utilized by both outer and inner active sites of the CoO nanowires/CC electrode, while at higher scan rate only outer active sites can participate in the redox reactions.¹² Fig. 4B shows the galvanostatic charge–discharge curves of the needle-like CoO nanowires/CC electrode between 0 and 0.45 V at various current densities. A symmetric shape during the charge–discharge process is observed, indicating their good supercapacitive behaviors. The specific capacitance is shown as a function of the current density (Fig. 4C). The specific capacitance of the needle-like CoO nanowires is 311.8 , 301.3 , 281.2 , 263.6 , 247.5 , and 232.9 F g^{-1} at 1 , 2 , 4 , 6 , 8 , and 10 A g^{-1} current density, respectively. This suggests that about 74.7% of the specific capacitance at 1 A g^{-1} is still retained when the discharge current density is increased to 10 A g^{-1} . Because a long cycling performance is one of the most important criteria for a SCs, the cycling lifetime tests over 1000 cycles for the needle-like CoO nanowire/CC electrode were carried out at 6 A g^{-1} . It is found that the needle-like CoO nanowire/CC electrode exhibits an excellent long-term electrochemical stability, and the capacitance loss after 1000 cycles is only 1.7% , as shown in Fig. 4D. Besides, the electrochemical properties of needle-like CoO nanowires/CC product was also studied at the bending state. Fig. 4E shows the CVs of the flexible supercapacitors with a planar state and the bending state at a fixed scan rate of

20 mV/s. Obviously, the CV curves of this flexible electrode was almost overlapped when testing at a planar state and the bending state. The electrochemical impedance spectroscopy (EIS) measurements are employed to further evaluate the electrochemical properties of needle-like CoO nanowires/CC electrode at a planar state and the bending state. Fig. 4F shows the Nyquist plot for the needle-like CoO nanowires/CC structure at a planar state and the bending state, which consist of semicircle arcs at high-to middle frequency region and straight lines at low frequency range. The diameter of semicircular arc and the slope of the straight lines are nearly the same, which demonstrated its excellent mechanical stability as flexible energy storage devices.

In summary, needle-like cobalt oxides nanowires supported on the CC were successfully prepared by a hydrothermal method and subsequent post-annealing treatment. The needle-like CoO nanowires supported on the CC exhibited a specific capacitance of 311.8 F g⁻¹ at 1 A g⁻¹ and an outstanding specific capability retention of 74.7% with a 10 times current density increase from 1 to 10 A g⁻¹. The excellent long-term cycle stability over 1000 cycles and no obvious decrease at 6 A g⁻¹ were also achieved. In comparison with Co₃O₄ nanowires/CC, CoO nanosheets/CC and CoO microspheres, needle-like CoO nanowires supported on the CC indicates much enhanced electrochemical performances. This work provides a promising method to fabricate needle-like CoO nanowires supported on the CC for the improved electrochemical performance as attractive electrode materials in the field of supercapacitors.

This work is supported by National Natural Science Foundation of China (51372279), Hunan Provincial Natural Science Foundation of China (13JJ1005) and Shenghua Scholar Program of Central South University.

Notes and references

^a Department of Inorganic Materials, Central South University, Changsha, Hunan 410083, P. R. China.

E-mail: liuxh@csu.edu.cn; chenlimiao@csu.edu.cn

^b School of Materials Science and Engineering, Central South University, Changsha, Hunan 410083, P. R. China.

^c State Key Laboratory of High Performance Complex Manufacturing, School of Mechanical and Electrical Engineering, Central South University, Changsha, Hunan 410083, P. R. China.

E-mail: lijunhui@csu.edu.cn

^d Institute for Materials Microstructure, Central South University, Changsha, Hunan 410083, P. R. China.

† Electronic Supplementary Information (ESI) available: [details of any supplementary information available should be included here]. See DOI: 10.1039/b000000x/

- 1 (a) G. Wang, L. Zhang and J. Zhang, *Chem. Soc. Rev.*, 2012, **41**, 797; (b) Y. He, W. Chen, C. Gao, J. Zhou, X. Li and E. Xie, *Nanoscale*, 2013, **5**, 8799; (c) X. Peng, L. Peng, C. Wu and Y. Xie, *Chem. Soc. Rev.*, 2014, **43**, 3303.
- 2 C. C. Hu, K. H. Chang, M. C. Lin, and Y. T. Wu, *Nano Lett.*, 2006, **6**, 2690.
- 3 C. Yuan, X. Zhang, and L. Su, *J. Mater. Chem.*, 2009, **19**, 5772.
- 4 (a) J. Liu, J. Jiang, C. Cheng, H. Li, J. Zhang, H. Gong, and H. J. Fan, *Adv Mater.*, 2011, **23**, 2076; (b) C. Zhou, Y. Zhang, Y. Li and J. Liu, *Nano Lett.*, 2013, **13**, 2078.
- 5 M. B. Toupin, T. Belanger, D. Chem. Mater., 2004, **16**, 3184.
- 6 H. Wang, H. S. Casalongue, Y. Liang, and H. Dai, *J. Am. Chem. Soc.*, 2010, **132**, 7472.
- 7 X. Liu, R. Ma, Y. Bando and T. Sasaki, *Adv. Mater.*, 2012, **24**, 2148.
- 8 (a) Q. Guan, J. Cheng, B. Wang, W. Ni, G. Gu, X. Li, L. Huang, G. Yang and F. Nie, *ACS Appl. Mater. Inter.*, 2014, **6**, 7626; (b) X. H. Xia, J. P. Tu, X. L. Wang, C. D. Gu and X. B. Zhao, *Chem. Commun.*, 2011, **47**, 5786; (c) C. Cheng, G. Zhou, J. Du, H. Zhang, D. Guo, Q. Li, W. Wei and L. Chen, *New J. Chem.*, 2014, **38**, 2250.
- 9 D. Lan, Y. Chen, P. Chen, X. Chen, X. Wu, X. Pu, Y. Zeng and Z. Zhu, *ACS Appl. Mater. Inter.*, 2014, **6**, 11839.
- 10 R. S. Devan, R. A. Patil, J.-H. Lin and Y.-R. Ma, *Adv. Funct. Mater.*, 2012, **22**, 3326.
- 11 M. V. Reddy, G. Prithvi, K. P. Loh and B. V. Chowdari, *ACS Appl. Mater. Inter.*, 2014, **6**, 680.
- 12 C. Guan, J. Liu, C. Cheng, H. Li, X. Li, W. Zhou, H. Zhang and H. J. Fan, *Energy Environ. Sci.*, 2011, **4**, 4496.
- 13 W. Xing, S. Qiao, X. Wu, X. Gao, J. Zhou, S. Zhuo, S. B. Hartono and D. Hulicova-Jurcakova, *J. Power Sources*, 2011, **196**, 4123.
- 14 R. B. Rakhi, W. Chen, D. Cha and H. N. Alshareef, *Nano Lett.*, 2012, **12**, 2559.
- 15 (a) S. Cheng, L. Yang, Y. Liu, W. Lin, L. Huang, D. Chen, C. P. Wong and M. Liu, *J. Mater. Chem. A*, 2013, **1**, 7709; (b) L. Shen, Q. Che, H. Li and X. Zhang, *Adv. Funct. Mater.*, 2014, **24**, 2630; (c) D. Zhang, H. Yan, Y. Lu, C. W. Kangwen Qiu, C. Tang, Y. Zhang, C. Cheng and Y. Luo, *Nanoscale Res. Lett.*, 2014, **9**, 139.
- 16 B. Liu, J. Zhang, X. Wang, G. Chen, D. Chen, C. Zhou and G. Shen, *Nano Lett.*, 2012, **12**, 3005.
- 17 (a) L. Yu, G. Zhang, C. Yuan and X. W. Lou, *Chem. Commun.*, 2013, **49**, 137; (b) X. Liu, R. Ma, Y. Bando and T. Sasaki, *Adv. Funct. Mater.*, 2014, **24**, 4292.
- 18 W. Li, X. Wang, B. Liu, S. Luo, Z. Liu, X. Hou, Q. Xiang, D. Chen and G. Shen, *Chem. Eur. J.*, 2013, **19**, 8650.